

Picophotonics - Subatomic Optical Resolution Beyond Thermal Fluctuations

Tongjun Liu¹, Jun-Yu Ou¹, Jie Xu¹, Eng Aik Chan², Kevin F. MacDonald¹, and Nikolay I. Zheludev^{1,2}

¹ *Optoelectronics Research Centre and Centre for Photonic Metamaterials, University of Southampton, Highfield, Southampton, SO17 1BJ, UK*

² *Centre for Disruptive Photonic Technologies, SPMS and TPI, Nanyang Technological University, Singapore, 637378, Singapore*

Despite recent tremendous progress in optical imaging and metrology, the resolution gap between atomic scale transmission electron microscopy and optical techniques has not been closed. Is optical imaging and metrology of nanostructures exhibiting Brownian motion possible with resolution beyond thermal fluctuations? Here we report on an experiment in which the average position of a nanowire with a thermal oscillation amplitude of ~ 150 pm is resolved in single-shot measurements with absolute error of ~ 30 pm using light at a wavelength of $\lambda = 488$ nm, providing the first example of such sub-Brownian metrology with $\lambda/10,000$ resolution. To localize the nanowire, we employ a deep learning analysis of the scattering of topologically structured light, which is highly sensitive to the nanowire's position. As a non-invasive optical metrology with sub-Brownian absolute errors, down to a fraction of the typical size of an atom (Si: 220 pm diameter), it opens the exciting field of picophotonics.

Over the past decade, spatial resolution in far-field optical imaging and metrology has improved far beyond the classical Abbe diffraction limit of $\lambda/2$, where λ is the wavelength of light. Nonlinear STED (stimulated emission depletion) and statistically enhanced STORM (stochastic optical reconstruction microscopy) techniques used in biological imaging^{1,2} now routinely achieve resolution of a few tens on nanometers, or better than $\lambda/10$. The application of artificial intelligence to the analysis of coherent light scattered by an object offers metrology with an accuracy of only a few nanometers, or better than $\lambda/100$ ³, on a par with scanning electron microscopy. In what follows, we demonstrate an approach to optical measurements with absolute error reaching a previously unimaginable level of $\lambda/10,000$ – a “sub-Brownian” length scale, equivalent to a fraction of the typical size of an atom, and several times shorter than the thermal motion amplitude of the target objects and the resolution of transmission electron (cryo)microscopy. In single-shot measurements we determine object dimensions through a deep learning-enabled analysis of its scattering pattern when it is illuminated with coherent, topologically structured light containing deeply subwavelength singularity features.

In experiment, we measure the in-plane position of a suspended nanowire, cut by focused ion beam milling from a 50 nm thick Si_3N_4 membrane coated with 65 nm gold, relative to a fixed edge of the surrounding membrane (Fig. 1). This position, i.e. the width of the gap between the nanowire and the membrane edge, could be controlled electrostatically with high precision over a few nanometer range through the application of a DC

bias across the gap. The sample was illuminated by a coherent light at a wavelength of $\lambda = 488$ nm, with either a plane (defocused Gaussian) wavefront or a superoscillatory wavefront profile formed by a spatial

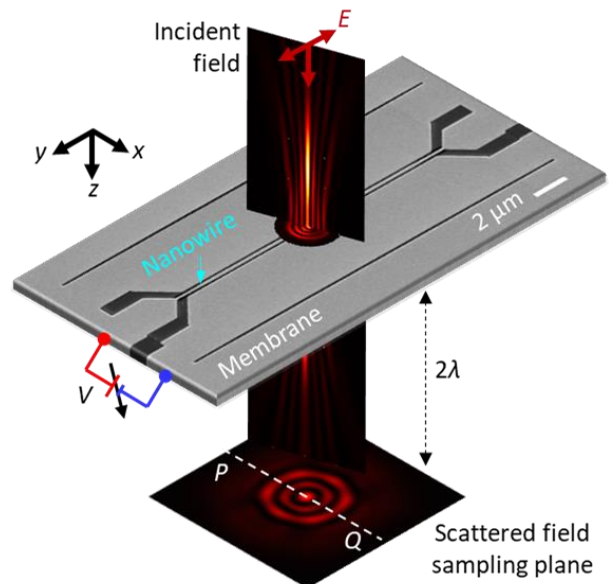


Fig. 1. Measuring nanowire displacement via scattering of topologically structured light. Incident light scattered from the nanowire (in the present case, 17 μm long and 200 nm wide with a 100 nm gap on either side) is imaged in transmission through a high-NA microscope objective (not shown). Deeply-subwavelength lateral (x -direction) displacements of the wire, controlled by application of a DC bias between the wire and the adjacent edge of the supporting membrane, are quantified via a deep-learning enabled analysis of single-shot scattering patterns.

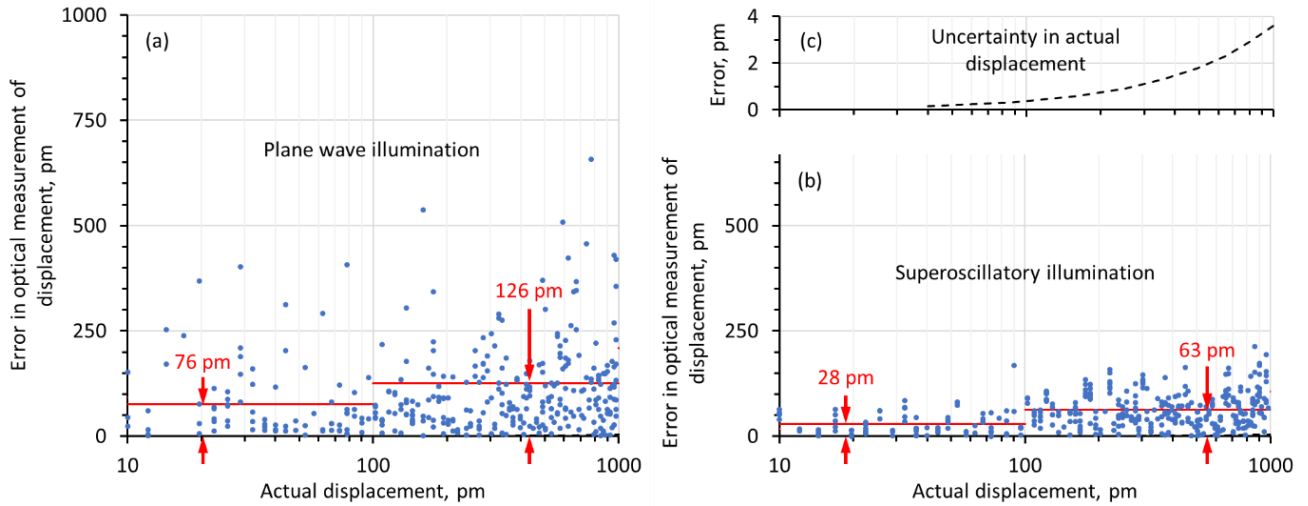


Fig. 2. Optical measurements of nanowire displacement. Absolute error in measurements of nanowire displacement, using (a) plane wave and (b) topologically structured (superoscillatory) light field illumination, against actual displacement. Red horizontal lines show mean absolute errors for order-of-magnitude actual displacement bands, i.e. from 10-100 and 100-1000 pm. (c) Magnitude of uncertainty in actual nanowire displacement.

light modulator-based wavefront synthesizer (see Supplementary Materials section S1). The pattern of light scattered by the nanostructure was sampled in transmission at a distance of $\sim 2\lambda$ ($\sim 1 \mu\text{m}$) from the membrane by a 16-bit image sensor through a microscope objective with a numerical aperture of 0.9.

To enable optical measurements of unknown nanowire positions, we created a dataset of single-shot scattering patterns recorded at different (electrostatically controlled) positions of the nanowire. Knowledge of said position being obtained from an *a priori* measurement, under a scanning electron microscope, of the dependence of nanowire position on applied bias. Eighty percent of these images, selected at random, were used for neural network training, i.e., as scattering patterns for known positions of the nanowire. (Detail of the network architecture and training procedure, and positional calibration measurements are given in Supplementary Materials section S2.) The trained network was then tasked with determining (nominally) unknown nanowire positions from previously unseen single-shot scattering patterns. This exercise was repeated for the two regimes of (plane wave and superoscillatory) illumination.

Figure 2 shows the results of such measurements, as the absolute error in the optical measurement of nanowire position, retrieved by the trained neural network from the scattering pattern, against the ground truth (*a priori* calibrated) displacement values in the 10-1000 pm range. The statistical spread of datapoints is derived from twenty independent neural network training cycles. Our results show that nanowire position can be measured with a mean absolute error of as little as 76 pm using plane wave illumination and 28 pm with superoscillatory illumination. For comparison, the diameter of a silicon atom is ~ 220 pm.

Optical metrology based upon analysis of scattered light is an inverse problem that can be reduced to the Fredholm integral equation, which can be efficiently solved by a neural network³. Recent work has demonstrated that this approach yields accuracy better than $\lambda/100$ in measuring the width of gaps in an opaque film with plane wave illumination, using a neural network trained on a set of nanofabricated samples with a range of different gap sizes. There are two major contributing factors to the hundredfold improvement in mean absolute error reported here: a radically better training process and the use of topologically structured superoscillatory light:

Precisely tailored interference of multiple waves can form intensity “hotspots” in free space, with dimensions smaller than the conventional diffraction limit, as a manifestation of what is known as superoscillation. The electromagnetic field near a superoscillatory hotspot has many features similar to those in the vicinity of resonant plasmonic nanoparticles or nanoholes - hotspots are surrounded by phase singularities and nanoscale zones of energy backflow where phase gradients can be more than an order of magnitude larger than in a free propagating plane waves⁴.

The use of such topologically structured light gives a radical advantage for AI-enabled metrology: The ability to evaluate small changes in the position of the nanowire depends upon the magnitude of associated changes in the scattered light field at distance z from the object $A(x, z)e^{i\phi(x)} = f(A_0(x, 0)e^{i\phi_0(x, 0)})$, where $A_0(x, 0)$ is the amplitude and $\phi_0(x, 0)$ is the phase of the incident light in the xy object plane. A small displacement in the object against the incident field in the x -direction results in a change in scattered light intensity $\delta I(x) \sim \delta A_0(x, 0)^2 + A_0(x, 0)^2 \delta \phi_0(x, 0)^2$. The first term in this expression is related to the change of

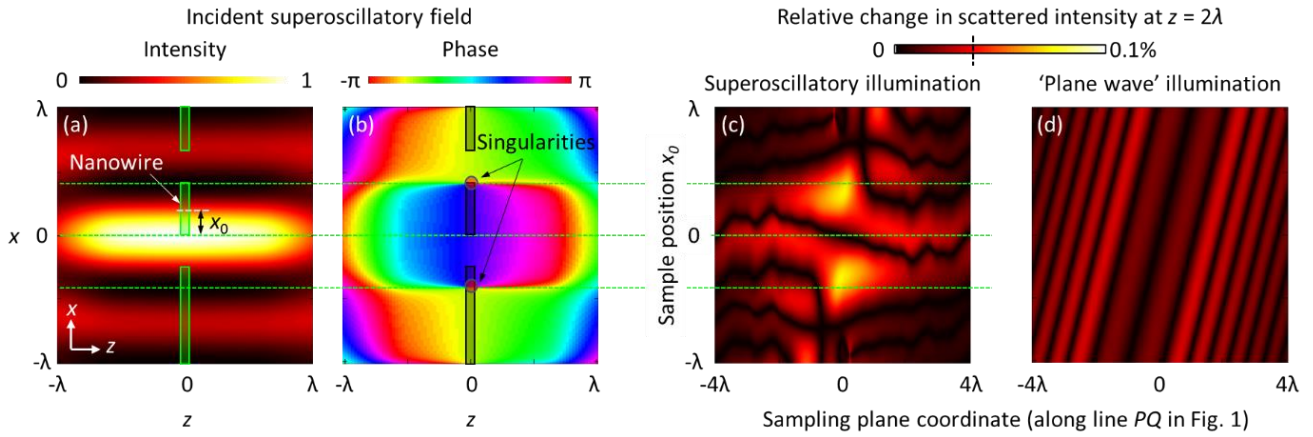


Fig. 3. Sensitivity of scattered fields to small nanowire displacements. (a) Intensity and (b) phase profiles of the superoscillatory field in the xz plane [light propagating in the $+z$ direction, wavelength $\lambda = 488$ nm]. The sample – a nanowire in the gap between two semi-infinite sections of membrane – lies in the $z = 0$ plane [its cross-sectional profile being shown in green in (a) and grey in (b)]. (c) Relative change in scattered light intensity resulting from a $\lambda/1000$ displacement of the sample in x -direction along a cross-sectional line through the scattering pattern in the sampling plane [the line PQ in Fig. 1] as a function of the initial position x_0 of the sample relative to the symmetry axis of the light field. (d) Corresponding plot of relative change in scattered light intensity for plane wave illumination of the same sample structure. [Further detail of numerical simulations is given in Supplementary information section S3.]

illumination intensity associated with the object's positional shift, while the second relates to the corresponding change in phase. The phase-dependent term is absent for plane wave illumination, but can be large under superoscillatory illumination, when the object traverses a small (deeply subwavelength) feature of the incident field, such as singularity, where the phase $\phi_0(x, 0)$ jumps by π .

The responses of scattered plane wave and topologically structured light fields to displacement of an illuminated nanowire are illustrated, through computational modelling, in Fig. 3. The incident superoscillatory wavefront (detailed in Ref. ⁴) has a central intensity maximum (Fig. 3a) flanked by phase singularities and zones of high phase gradient (Fig. 3b). We consider the case here where these singularities lie in the nanowire sample plane. As a figure of merit for the sensitivity of the scattered field to small displacements of the nanowire, Fig. 3c presents the magnitude of the relative change in scattered light intensity induced by a $\lambda/1000$ (~ 0.5 nm) shift in nanowire position, as a function of (horizontally) image plane coordinate and (vertically) the initial position of the sample within the structured light field. The scattered field intensity is strongly dependent on both, with largest changes (of up to 0.1%), occurring when a sharp edge of the nanostructure coincides with a phase singularity in the incident superoscillatory field. For comparison, Fig. 3d shows the same for plane wave illumination. Here, the variations in scattered field intensity are smaller (reaching only 0.03%) and relatively weakly dependent on both image plane coordinate and lateral position of the sample. The contrast between Figs. 3c and 3d explains the better mean error of positional measurement achieved with

superoscillatory, as compared to plane wave, illumination (Fig 2).

The quality of artificial intelligence is directly related to the quality of training data for the neural network. Our ability here to achieve picometric levels of absolute error results firstly from the use of a training set that is ultimately congruent with the object of interest: the same electrostatically reconfigurable nanostructure is used for training and as the object of metrological study. Moreover, ground truth positional displacement values are much more precisely calibrated in this singular electrostatically controlled gap sample (Fig. 2c) than they are in previously employed sets of mutually independent training samples fabricated with typically few-nanometer tolerance^{3,5}.

It should further be noted that access to this low level of measurement error is only possible because deep learning-based retrieval process is sensitive primarily to the intensity profile of the diffraction pattern, but not to its lateral position. As such it is strongly resilient to small thermal and mechanical drifts in the mutual positions of the lens, sample, and incident light beam during the experiment⁵.

Our results represent the first example of “sub-Brownian” optical metrology – the measurement of object dimensions/displacements smaller than the amplitude of its thermal motion. The amplitude of nanowire thermal vibration can be evaluated from the Langevin oscillator model ⁶: in the present case, the nanowire's fundamental in-plane oscillatory mode at 1.6 MHz has an amplitude of 145 pm at room temperature (see supplementary materials S4), i.e. a value markedly higher than the achieved (superoscillatory illumination) measurement error of ~ 30 pm. This is possible because

our measurements are performed with a detector integration time of ~ 100 ms and thus return the mean position of the nanowire, which oscillates thermally with a much shorter (~ 0.6 μ s) period. Measurements are single-shot, and do not require scanning of the object, so they can be performed in binning mode, with a frame rate equal to that of the image sensor, which may reach hundreds of megahertz.

AI-enabled analysis of scattering in topologically structured light fields offers access, under ambient conditions, to levels of resolution in optical imaging and measurement that are otherwise only attainable in (cryo-)electron and near-field scanning probe microscopies. Extreme resolution, surpassing the diffraction limit of conventional microscopes by a factor of ten thousand, has been demonstrated here on a system allowing for the collection of *in-situ* physical training data for the neural network. While a dependence on *in-situ* training is a limitation, it is applicable in many systems and the approach offers numerous practical applications, for example in: non-contact position monitoring of platforms in ultra-precise STM/AFM instruments; monitoring positional displacements in MEMS and NEMS devices such as accelerometers and nanomachines; monitoring structural deformations and thermal drifts in precise instruments (e.g. telescope mirrors) and seismographs; measuring the thermal expansions of macroscopic objects and monitoring nano-gaps affected by microkelvin temperature variations. The technique can be used in gravitational wave detectors based on monitoring test mass displacements or shape oscillations, and may be particularly relevant to emerging studies of quantum gravity with micro-masses⁷.

Moreover, non-invasive single-shot optical metrology with sub-Brownian resolution, which can be performed with high frame rate image sensors, opens up the exciting field of time-domain picophotonics, with exciting applications potential in applied research and fundamental science. This includes the study of Brownian motion thermodynamics of nano-objects, including the ballistic regime⁸ of thermal fluctuations, which may have applications in fast thermometry and mass measurement (where the fundamental thermodynamic connection between motion frequencies/amplitudes and the material/geometric parameters of the object would preclude the need for calibration against external standard); the study of quantum gravity⁷, Van Der Waals, optically-induced and (non-)Hamiltonian forces in nano-mechanics^{9,10}; electron and plasmon quantum transport through atomic scale gaps¹¹⁻¹³; configuration chemistry of individual molecules; protein folding¹⁴; and other dynamic events in macromolecules, nanomachines and 2D materials (where flexural, phononic modes are now understood to be of critical importance to thermal, electrical and mechanical properties¹⁵⁻¹⁹).

Acknowledgements

This work was supported by the Engineering and Physical Sciences Research Council, UK (grant numbers EP/M009122/1 and EP/T02643X/1; NIZ, KFM, JYO), the Ministry of Education, Singapore (MOE2016-T3-1-006; NIZ), and the China Scholarship Council (201806160012; TL).

Data availability

The data from this paper can be obtained from the University of Southampton ePrints research repository.

References

1. S. W. Hell and J. Wichmann, *Opt. Lett.* **19**, 780 (1994).
2. M. J. Rust, M. Bates and X. Zhuang, *Nat. Methods* **3**, 793 (2006).
3. C. Rendón-Barraza, E. A. Chan, G. Yuan, G. Adamo, T. Pu and N. I. Zheludev, *APL Photon.* **6**, 066107 (2021).
4. G. Yuan, E. T. F. Rogers and N. I. Zheludev, *Light Sci. Appl.* **8**, 2 (2019).
5. T. Pu, J. Y. Ou, V. Savinov, G. Yuan, N. Papasimakis and N. I. Zheludev, *Adv. Sci.* **8**, 2002886 (2020).
6. M. C. Wang and G. E. Uhlenbeck, *Rev. Mod. Phys.* **17**, 323 (1945).
7. M. Aspelmeyer, at *8th International Topical Meeting on Nanophotonics and Metamaterials*, Seefeld-in - Tirol, Austria, 2022.
8. T. Liu, J.-Y. Ou, K. F. MacDonald and N. I. Zheludev, at *Conference on Lasers and Electro-Optics 2021*, Virtual Conference, 2021.
9. M. V. Berry and P. Shukla, *Proc. R. Soc. A* **471**, 20150002 (2015).
10. A. W. Rodriguez, F. Capasso and S. G. Johnson, *Nat. Photon.* **5**, 211 (2011).
11. W. Zhu, R. Esteban, A. G. Borisov, J. J. Baumberg, P. Nordlander, H. J. Lezec, J. Aizpurua and K. B. Crozier, *Nat. Commun.* **7**, 11495 (2016).
12. J. J. Baumberg, J. Aizpurua, M. H. Mikkelsen and D. R. Smith, *Nat. Mater.* **18**, 668 (2019).
13. B. Yang, G. Chen, A. Ghafoor, Y. Zhang, Y. Zhang, Y. Zhang, Y. Luo, J. Yang, V. Sandoghdar, J. Aizpurua, Z. Dong and J. G. Hou, *Nat. Photon.* **14**, 693 (2020).
14. S. W. Englander and L. Mayne, *Proc. Natl. Acad. Sci.* **111**, 15873 (2014).
15. S. V. Morozov, K. S. Novoselov, M. I. Katsnelson, F. Schedin, D. C. Elias, J. A. Jaszczak and A. K. Geim, *Phys. Rev. Lett.* **100**, 016602 (2008).
16. E. Mariani and F. von Oppen, *Phys. Rev. Lett.* **100**, 076801 (2008).
17. A. Taheri, S. Pisana and C. V. Singh, *Phys. Rev. B* **103**, 235426 (2021).
18. L. Lindsay, D. A. Broido and N. Mingo, *Phys. Rev. B* **82**, 115427 (2010).
19. S. Zheng, J.-K. So, F. Liu, Z. Liu, N. Zheludev and H. J. Fan, *Nano Lett.* **17**, 6475 (2017).

Supplementary Information:

Picophotonics - Subatomic Optical Resolution Beyond Thermal Fluctuations

Tongjun Liu¹, Jun-Yu Ou¹, Jie Xu¹, Eng Aik Chan², Kevin F. MacDonald¹, and Nikolay I. Zheludev^{1,2}

¹ *Optoelectronics Research Centre and Centre for Photonic Metamaterials, University of Southampton, Highfield, Southampton, SO17 1BJ, UK*

² *Centre for Disruptive Photonic Technologies, SPMS and TPI, Nanyang Technological University, Singapore, 637378, Singapore*

S1: Wavefront synthesizer

The computer-controlled wavefront synthesizer employed in this work is described in detail in Ref. 1. It is based upon a pair of (Meadowlark P512) spatial light modulators – one for intensity and the other for phase modulation. In the present case, for laser light at a wavelength $\lambda = 488$ nm, it was programmed to generate an axially-symmetric superoscillatory wavefront constructed from two circular prolate spheroidal functions $E(r/\lambda) = 4.477 S_3(r/\lambda) + S_4(r/\lambda)$, where r is radial distance from the beam axis.

In the ‘plane wave’ illumination regime, the synthesizer was configured to generate a defocused Gaussian beam profile ² having a (measured) intensity variance of only $\pm 5\%$ over the ~ 400 nm width of the sample (i.e. including the nanowire and gap on either side).

S2: Neural network architecture, training, and application procedures

The neural network contained three convolution layers with, respectively, sixty-four 5×5 , one hundred and twenty-eight 4×4 , and two hundred and fifty-six 2×2 kernels, and three fully connected layers with 128, 256, 128 neurons. Each of the convolution layers was followed by a pooling layer with 4×4 , 3×3 , and 3×3 kernels with Rectified Linear Unit activation functions. The network was trained with the Adam stochastic optimization method and root mean square error loss function.

Our dataset comprised scattering intensity patterns imaged with a $9\lambda \times 9\lambda$ (350×350 pixels) field of view of at a distance 2λ from the sample. These were recorded (for each regime of illumination) at 201 different electrostatically-controlled positions of the nanowire, with x-direction displacements of ≤ 4 nm from its zero-bias equilibrium position. 64% of images (selected at random) were used for network training, 16% for validation, with the remaining 20% then employed for testing (i.e. as scattering patterns for nominally unknown nanowire positions, to be determined by the trained network). For statistical purposes, i.e. to exclude the dependence of measurement outcome on the selection of training images, and their order of appearance in the training set, twenty independent iterations of the training, validation and testing procedure were performed.

Ground truth values of nanowire displacement were independently established by a priori measurements under a scanning electron microscope for a number of different bias settings and interpolated by a quadratic dependence. Indeed, the first non-zero term in the analytical expression for the dependence of nanowire displacement on applied bias must be quadratic as displacement does not depend on the sign of the bias; and higher order terms are negligible while the magnitude of displacement remains much smaller than the gap size (~ 100 nm). Although each individual measurement by scanning electron microscope has an uncertainty of ± 1.2 nm, a large number of

measurements over a range of applied bias values enables determination of the quadratic dependence with high precision. Error propagation analysis yields an uncertainty in ground truth displacements of <0.4% of its value (as shown in Fig. 2c).

S3: Numerical modelling

Numerical simulations were performed using Lumerical FDTD Solutions. Silicon nitride is taken to have a refractive index $n = (2 + 0i)$, while parameters for gold are those by Johnson & Christy. Incident light is polarized parallel to the nanowire and perfectly matching layer (PML) boundary conditions are used. The incident superoscillatory field was generated through a binary amplitude mask as detailed in Ref. 3.

S4: Thermal fluctuations of the nanowire

The thermal motion of nanomechanical structures can be described by the Langevin model⁴. For a harmonic oscillator

$$\ddot{x} + \gamma\dot{x} + \omega_0^2 x = F_T(t)/m_{eff}$$

where

- $F_T(t) = \sqrt{2k_B T \gamma / m_{eff}} \eta(t)$ is the thermal force [which is related to the dissipation factor γ through the fluctuation-dissipation theorem⁵];
- k_B is the Boltzmann constant;
- T is temperature;
- $\eta(t)$ is a delta-correlated normalized white noise term: $\langle \eta(t) \rangle = 0$; $\langle \eta(t) \eta(t') \rangle = \delta(t - t')$;
- $\omega_0 = 2\pi f_0 = \sqrt{k/m_{eff}}$ is the natural angular frequency of oscillation, f_0 being the natural frequency and k the spring constant;
- and m_{eff} is the oscillator's effective mass;

the RMS beam displacement is

$$\delta x_{RMS} = \sqrt{k_B T / (4\pi^2 m_{eff} f_0^2)}$$

In the present case, $f_0 = 1.6$ MHz and $m_{eff} = 2$ pg, giving an average thermal fluctuation amplitude of ~145 pm.

References

1. E. T. F. Rogers, S. Quraishie, K. S. Rogers, T. A. Newman, P. J. S. Smith and N. I. Zheludev, *APL Photon.* **5**, 066107 (2020).
2. C. Rendón-Barraza, E. A. Chan, G. Yuan, G. Adamo, T. Pu and N. I. Zheludev, *APL Photon.* **6**, 066107 (2021).
3. G. Yuan, E. T. F. Rogers and N. I. Zheludev, *Light Sci. Appl.* **8**, 2 (2019).
4. M. C. Wang and G. E. Uhlenbeck, *Rev. Mod. Phys.* **17**, 323 (1945).
5. R. Kubo, M. Toda and N. Hashitsume, *Statistical Physics II: Nonequilibrium Statistical Mechanics.* (Springer, Berlin, 1991).